Laser-wavelength and intensity dependence of electron-nuclear energy sharing in dissociative ionization of H_2

Chaoxiong He,[1] Hao Liang,[1] Ming-Ming Liu,[1] Liang-You Peng,[1,2,3,*] and Yunquan Liu[1,2,3,†]

[1]*State Key Laboratory for Mesoscopic Physics and School of Physics, Peking University, Beijing 100871, China*

[2]*Collaborative Innovation Center of Quantum Matter, Beijing 100871, China*

[3]*Collaborative Innovation Center of Extreme Optics, Shanxi University, Taiyuan, Shanxi 030006, China*

(Received 29 September 2019; accepted 8 April 2020; published 4 May 2020)

We experimentally and theoretically study the photoelectron-nuclear energy sharing mechanism of the correlated dynamics between the photoelectrons and the fragmented ions in the dissociative ionization of H_2 with respect to the laser intensity at the wavelengths $\lambda = 395$ nm and $\lambda = 790$ nm. We show that the prominent photoelectron-nuclear energy sharing along the back-diagonal lines is only observed for 395 nm at lower intensities, which is absent for increased intensities at 395 nm and for 790 nm lasers over a wide range of intensities. Based on a quantum mechanical model that includes the correlation between the photoelectron and the parent ion, we show that bond hardening has a significant effect on the photoelectron-nuclear energy sharing. The resonant states of the neutral hydrogen molecule during strong-field ionization and the distribution of vibrational states of molecular ions determine the joint energy spectrum of photoelectrons and nuclei. The study provides an intuitive and comprehensive description and understanding of the correlated photoelectron-nuclear dynamics in the dissociative ionization.

DOI: 10.1103/PhysRevA.101.053403

I. INTRODUCTION

The dynamical interaction between strong laser pulses and atoms or molecules is one of the most complicated and interesting topics in ultrafast physics. These essential interactions involve the energy and momentum exchange among the photons, the photoelectrons, and the nuclei. In particular, the electrons can absorb an excess number of photons, resulting in equally distributed peaks separated by the energy of one photon in the photoelectron energy spectrum, which is referred to as above-threshold ionization (ATI) [1]. For molecules, besides the ATI process, owing to the complex electronic states and the vibrational/rotational motions of the nuclei, many additional interesting phenomena may take place, such as bond softening [2], bond hardening [3], above threshold dissociation [4], and charge resonant enhanced ionization [5], etc.

For the simplest diatomic molecule H_2, how the excess energy is shared during photoionization between the nuclei and the photoelectron has been intriguing in the laser-molecule interaction. The partition process can be directly revealed in the joint energy spectrum (JES) of photoelectrons and kinetic energy release of nuclei, which reflects the dissociative ionization yields as a function of both the photoelectron energy E_e and the total nuclear energy $E_N = E_H + E_{H^+}$. The photoelectron-nuclear energy sharing has been experimentally observed using ultraviolet pulse at 390 nm [6] and x-ray synchrotron lasers [7]. For the complicated many-electron molecules, the photoelectron-nuclear energy sharing of CO molecules was shown to depend on the vibrational states [8] and the excited electronic states [9]. Theoretical studies [10,11] on the correlated photoelectron-nuclear dynamics for the ionization of H_2^+ under lasers with different wavelengths and intensities demonstrated that the JES structure has different features in the multiphoton ionization and the tunneling ionization regimes. However, the underlying mechanism of the energy sharing dependence on the laser parameters remains unclear and there is no experimental exploration.

Usually, the dissociative ionization of H_2 is described within a two-step scenario, i.e., the single ionization of H_2 and the subsequent dissociation of H_2^+. The two-step scenario provides a qualitative picture to analyze the interactions between H_2 and laser fields, as illustrated in Figs. 1(a) and 1(b). The heavy solid black curves stand for the lowest involved Born-Oppenheimer potential energy curves of H_2 and H_2^+ [12–14]. Here, we consider the laser induced deformation of the potential energy curves. One can get the adiabatic dressed potential energy curves by diagonalizing the Hamiltonian at a fixed internuclear distance $\hat{H}_F = \begin{pmatrix} E_g & 0 \\ 0 & E_u \end{pmatrix} + \frac{\hat{a}+\hat{a}^\dagger}{2}\begin{pmatrix} 0 & \mu F_0 \\ \mu F_0 & 0 \end{pmatrix} + \hat{N}\omega$, where F_0 and μ are, respectively, the amplitude of the laser field and the electric dipole moment, and $\hat{a}$, $\hat{a}^+$ and $\hat{N}$ represent the creation, annihilation, and the number operator of the photon field. We have calculated the adiabatic dressed potential energy curves with respect to the laser intensities at $\lambda = 395$ nm and $\lambda = 790$ nm, as shown in Figs. 1(a) and 1(b).

In Fig. 1(a), at $\lambda = 395$ nm, the potential energy curves of the lowest states of H_2^+ are both bent, and thus a barrier appears near the one photon resonance point near $R \approx 4$ a.u. and the height of the barrier lies on the laser intensity.

*liangyou.peng@pku.edu.cn

†yunquan.liu@pku.edu.cn

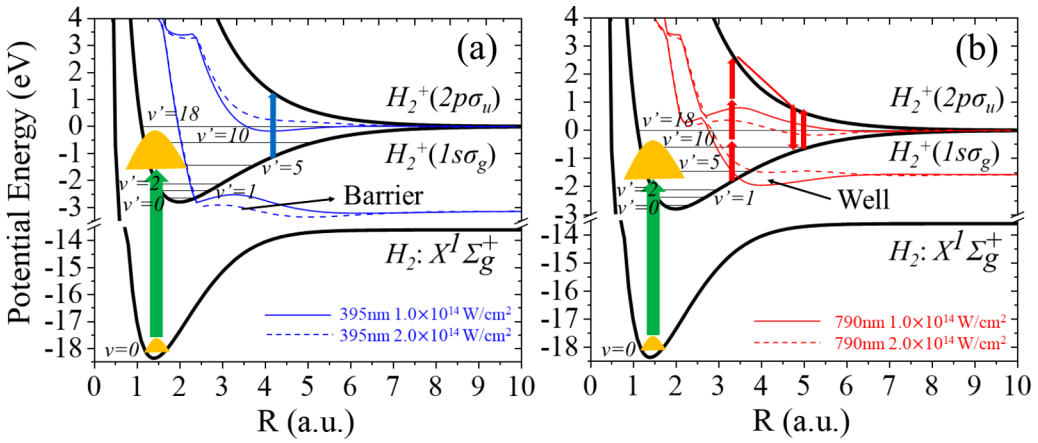

FIG. 1. The potential energy curves of H_2 and H_2^+. Heavy solid black curves in (a) and (b) are the diabatic potential energy curves. The thin blue or red curves in (a) and (b) are adiabatic dressed potential energy curves of H_2^+ at $\lambda = 395$ nm and at $\lambda = 790$ nm, respectively.

However, in Fig. 1(b), at $\lambda = 790$ nm, when the laser intensity is as high as 1.0×10^{14} W/cm^2, the potential energy curve is bent downward and a potential well is formed, thus the dressed state becomes a weakly bound state to a certain degree. Due to the quite different laser induced deformation of the potential energy curves and subsequent different dynamical processes at the two wavelengths, the photoelectron-nuclear energy sharing will sensitively depend on the laser wavelength and laser intensity.

In this paper, we experimentally and theoretically study the photoelectron-nuclear energy sharing in their correlated dynamics in the dissociative ionization of H_2 with respect to laser intensities at the wavelengths $\lambda = 395$ nm and $\lambda = 790$ nm. We present the unambiguous observation that the energy sharing between the photoelectron and the nuclei sensitively depends on the wavelength and the intensity of the driving laser field. Based on a quantitative model including the correlation between the photoelectron and the molecular ion, we show that the process of bond hardening has significant effects on the photoelectron-nuclear energy sharing at $\lambda = 790$ nm, while bond hardening hardly affects the energy sharing at $\lambda = 395$ nm. The resonant electronic states of the neutral hydrogen molecule in the multiphoton ionizations and the distributions of vibrational states of molecular ions determine the dynamics of the photoelectron-nuclear energy sharing of strong-field molecular dissociation.

II. EXPERIMENTAL RESULTS

Experimentally, linearly polarized 25-fs laser pulses at $\lambda = 790$ nm, are generated by the commercial Ti: Sapphire laser. The laser pulses at $\lambda = 395$ nm are generated with the barium borate crystal through the second harmonic process. The photoelectrons and dissociative ions are coincidently measured with the Cold Target Recoil Ion Momentum Spectroscopy (COLTRIMS) [15]. The momenta of the neutral hydrogen atoms are reconstructed according to the momentum conservation law $\vec{p}_e + \vec{p}_H + \vec{p}_{H^+} = 0$.

In Figs. 2(a) and 2(b), we show the measured intensity-dependent JESs at $\lambda = 395$ nm. As expected, for the lower intensity at $\lambda = 395$ nm, the general feature of JES is distributed as the back-diagonal lines reflecting a clear energy sharing mechanism, which was experimentally observed in Ref. [6]. The back-diagonal lines reveal the energy conservation law $E_N + E_e + U_p = E_0 + n\hbar\omega$, where E_0 and U_p stand for the initial bound energy of neutral H_2 and the ponderomotive energy, respectively. However, as the laser intensity increases to nearly 2.0×10^{14}W/cm^2 at $\lambda = 395$ nm, the structures of JESs evidently change from the back-diagonal to a nondiagonal horizontal distribution.

In Figs. 2(c) and 2(d), we show the corresponding photoelectron energy spectra at $\lambda = 395$ nm. For the lower intensity, there exist a difference about 1 eV between the single and the dissociative ionization channels. By increasing the laser intensity, the difference between those two channels becomes smaller and even harder to distinguish. The energy sharing between the nuclei and photoelectron is not evident and they would take the absorbed photons energy individually.

At $\lambda = 790$ nm, there is no such a similar diagonal tendency over a wide range of laser intensity about $0.9-2.2 \times 10^{14}$ W/cm^2, and the measured JESs always remain horizontal distributions as shown in Figs. 3(a) and 3(b). There does not exist clear evidence for the energy sharing between the photoelectron and the nuclei. As the laser intensity increases, the dominant dissociation channel changes from the one-photon pathway to the net-two-photon pathway. As shown in Figs. 3(c) and 3(d), the photoelectron energy spectra of the two channels are nearly identical, which is very different from those at $\lambda = 395$ nm. There is the relative yield enhancement near zero momentum of single ionization channel if compared with the dissociative ionization channel, which has reported in Ref. [16] and was attributed to the influence of autoionization.

III. THEORETICAL ANALYSIS

It has been shown that the vibrational states play a great importance in the photoelectron-nuclear correlation dynamics [17–20]. By ignoring the dependence of the ionization rates of H_2 on the internuclear distance and the subsequent dissociation of H_2^+, Franck-Condon transition can approximately describe the vibrational distributions of H_2^+ produced by single ionization of H_2 [21,22], which usually serves as the initial condition in the theoretical analysis of the dissociative ionization of H_2. However, experiments in Ref. [18–20] show

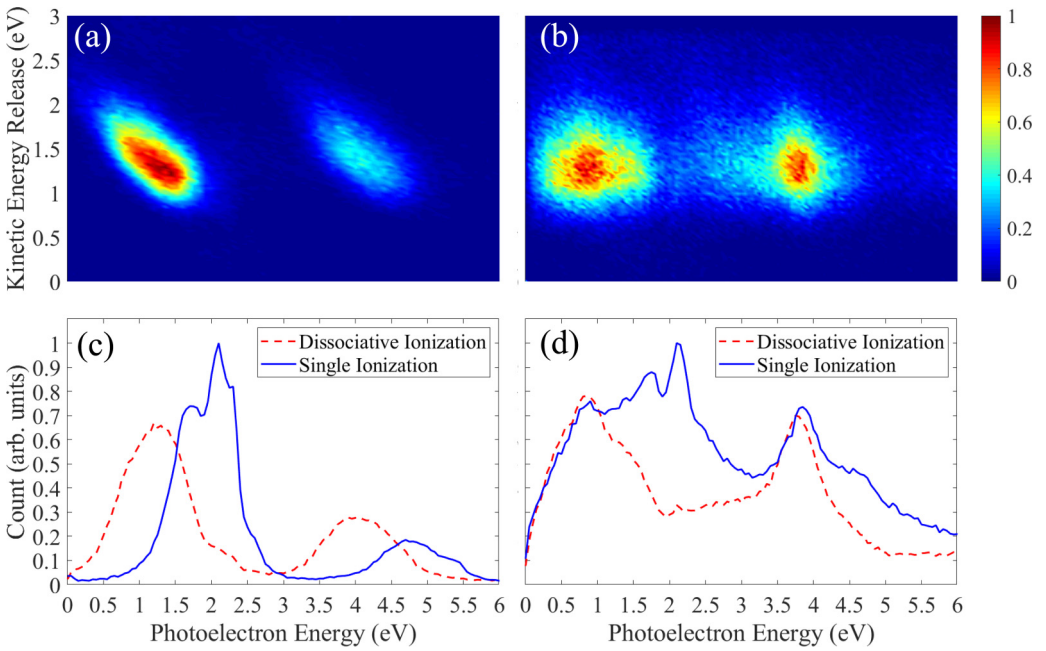

FIG. 2. (a), (b) the joint energy spectra measured at $\lambda = 395$ nm for different laser intensities. (c), (d) the photoelectron energy spectra corresponding to the dissociative and the single ionization channels. (a), (c) $I = 1.0 \times 10^{14}$ W/cm^2; (b), (d) $I = 1.96 \times 10^{14}$ W/cm^2.

that the vibrational distributions are critically dependent on laser parameters. In addition, for the homonuclear diatomic molecules, the laser field merely couples the motion of the electron relative to the nuclear center of mass without a direct coupling to the nuclei [23]. As it is known, currently it is not feasible to solve the time-dependent Schrödinger equation (TDSE) of strong-field dissociative H_2 molecules with both the electrons and the nuclei equally considered. Based on the statements above, one needs an explicit theory including the correlation and evolution of these particles in the laser field.

In order to analyze the laser wavelength- and intensity-dependent energy sharing behavior, we develop a quantitative model of molecular dissociation based on the strong field approximation. In this model, we remove the degree of the electron motion in TDSE, but keep the correlation between the ionized electron and the parent dissociative molecular ion.

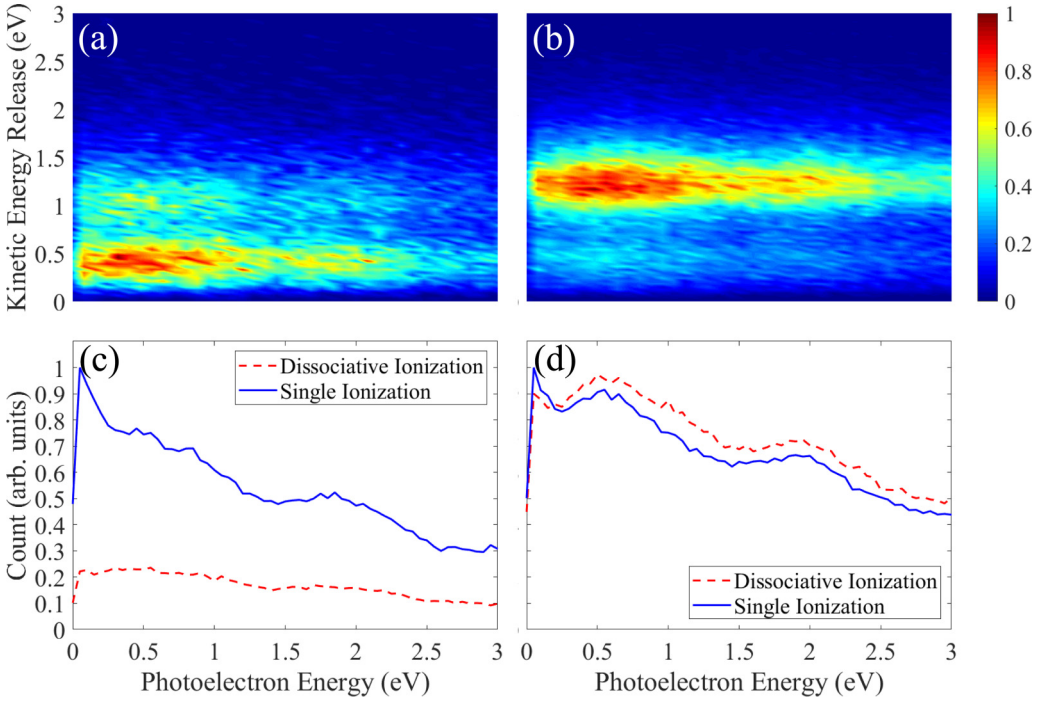

FIG. 3. (a),(b) the joint energy spectra measured at $\lambda = 790$ nm for different laser intensities. (c), (d) the photoelectron energy spectra corresponding to the dissociative and the single ionization channels. (a), (c) $I = 0.93 \times 10^{14}$ W/cm^2; (b), (d) $I = 2.20 \times 10^{14}$ W/cm^2.

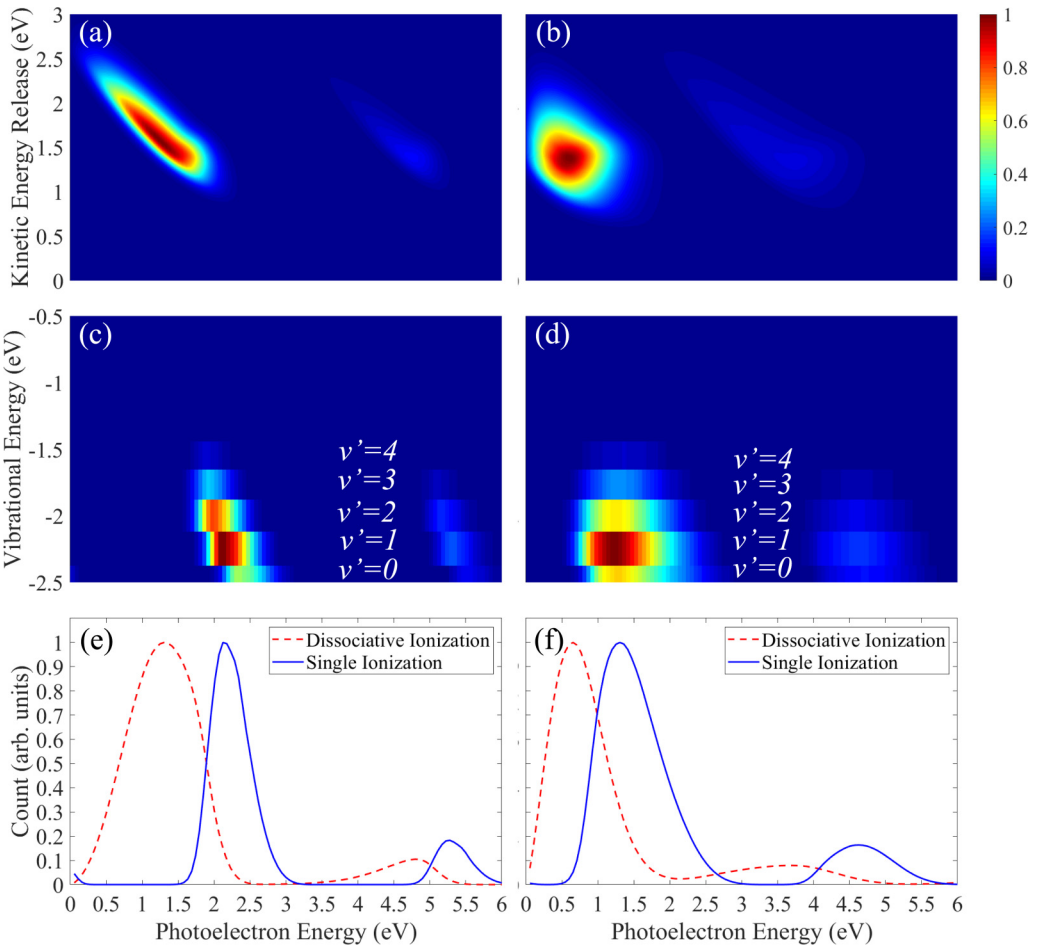

FIG. 4. (a) and (b) are the calculated joint energy spectra at $\lambda = 395$nm for different laser intensities. (c) and (d) are the energy of populated vibrational states with respect to the photoelectron energy. (e) and (f) are the calculated photoelectron energy spectra of the single ionization and the dissociative ionization channels. (a), (c) and (e) $I = 1.0 \times 10^{14}\,\mathrm{W/cm^2}$; (b), (d) and (f) $I = 2.0 \times 10^{14}\,\mathrm{W/cm^2}$.

To calculate the transition amplitude from the ground state $|0\rangle$ of H_2 to a certain state $|X, p_e\rangle$ with the state $|X\rangle$ for H_2^+ and the momentum p_e for the ionized electron, all one needs to do is to solve the following TDSE for H_2^+:

$$\left[i\partial_t - H_{H_2^+}(t) - \tfrac{1}{2}(p_e + A(t))^2 - E_0\right]|\Psi(t)\rangle = |f(t; p_e)\rangle,$$

with an inhomogeneous term $|f(t; p_e)\rangle = \sum_Y |Y\rangle\langle Y, p_e|V_{\mathrm{int}}(t)|0\rangle$ and the initial condition $|\Psi(t_i)\rangle = 0$, where $\{|Y\rangle\}$ is a complete orthonormal basis of H_2^+. The transition amplitude is given by $\langle X, p_e|U(t_f, t_i)|0\rangle = \langle X|\Psi(t_f)\rangle$. As is shown in the two-step scenario, the dynamics of H_2^+ is treated as a nuclear wave packet moving on the potential energy curves of its lowest two electronic states. According to whether the state $|X\rangle$ belongs to the bound state of H_2^+ or the continuum state corresponding to $H^+ + H$, one can distinguish the single ionization and the dissociative ionization channels. Detailed theoretical derivation is published elsewhere [24].

In Figs. 4(a) and 4(b), we present the calculated JESs at $\lambda = 395\,\mathrm{nm}$ at the intensities of $I = 1.0 \times 10^{14}\,\mathrm{W/cm^2}$ and $I = 2.0 \times 10^{14}\,\mathrm{W/cm^2}$, respectively. The energy sharing between photoelectrons and nuclei is only evident when the laser intensity is much lower. Since our model has the advantage of distinguishing the single ionization and dissociative ionization channels, we have analyzed the energy of populated vibrational states with respect to the energy of the emitted photoelectron, as shown in Figs. 4(c) and 4(d). The calculated photoelectron energy spectra from those two channels are shown in Figs. 4(e) and 4(f). The calculations well reproduce the experimental observations at $\lambda = 395\,\mathrm{nm}$. For the single ionization channel, one observes that H_2^+ wave packets are mostly populated on the lowest 3 vibrational levels with a clear upper boundary, and correspondingly the kinetic energy release mainly distributes at energies higher than a certain lower boundary near 1eV for the dissociative ionization channel.

In order to understand the intensity-dependent phenomenon at $\lambda = 395\,\mathrm{nm}$, we turn to the adiabatic Floquet theorem [2,25,26]. The H_2^+ wave packets below the barrier tend to remain bound and thus the barrier serves as the threshold of the fragmentation of H_2^+. The population of vibrational states is sensitively modulated if the laser intensity is increased. As the laser intensity increases, the barrier of the modified potential curve will decrease, which allows some wave packets bound at lower intensities to jump to the dressed $2p\sigma_u$ with a certain probability. Consequently, more vibrational wave packets will contribute to the dissociative ionization channels at higher intensities. Our calculations show that the JES of

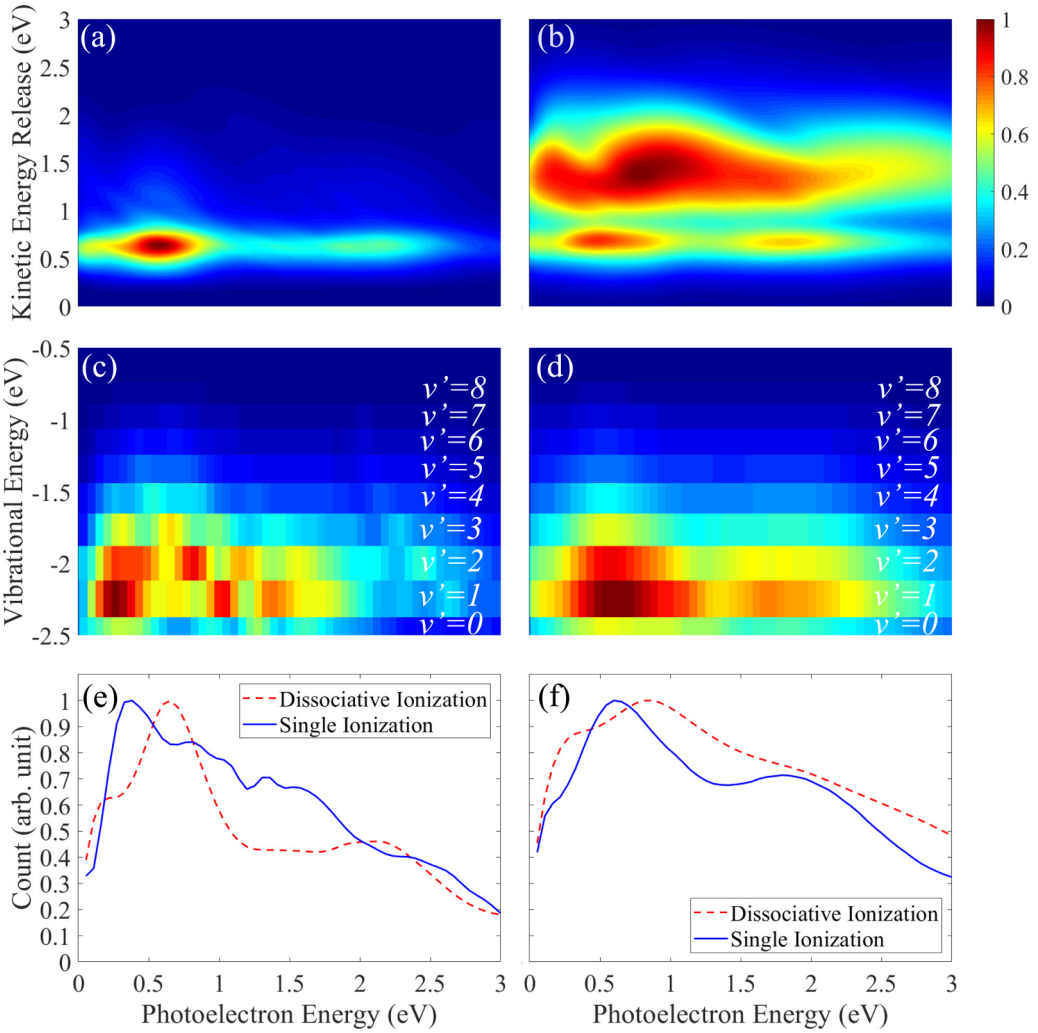

FIG. 5. (a) and (b) are the calculated joint energy spectra at $\lambda = 790$ nm for different laser intensities. (c) and (d) are the energy of populated vibrational states with respect to the photoelectron energy. (e) and (f) are the calculated photoelectron energy spectra of the single ionization and the dissociative ionization channels. (a), (c) and (e) $I = 1.0 \times 10^{14}\,\mathrm{W/cm^2}$; (b), (d) and (f) $I = 2.0 \times 10^{14}\,\mathrm{W/cm^2}$.

the dissociative ionization channel becomes much wider when the laser intensity is about $I = 2.0 \times 10^{14}\,\mathrm{W/cm^2}$ at $\lambda = 395$ nm, and the difference between the photoelectron energy spectra becomes smaller, as seen in Fig. 4(f). Therefore, the back-diagonal structures in JESs are blurred when the laser intensity become higher.

At $\lambda = 790$ nm, the calculated JESs reveal the nondiagonal horizontal structures at the intensities of $1.0 \times 10^{14}\,\mathrm{W/cm^2}$ and $2.0 \times 10^{14}\mathrm{W/cm^2}$, as shown in Figs. 5(a) and 5(b). As to the single ionization channel, the residual $H_2{}^+$ ions are mostly populated at the vibrational levels $v' = 0{-}5$, and the vibrational distribution is much wider than that at $\lambda = 395$ nm, as seen in Figs. 5(c) and 5(d).

In order to uncover the physical origins of the nondiagonal horizontal distribution of JES at $\lambda = 790$ nm, one must analyze the dissociative motion of the $H_2{}^+$ wave packets in the envelope of the laser pulse. Through a Landau-Zener tunneling [27–29], the $H_2{}^+$ wave packets near the barrier of the dressed potential curve may jump to the upper state and can be trapped during the interaction with the strong laser field. This opposite process to bond softening is named bond hardening [3,25]. Considering the dynamics of bond hardening, one can see that the $H_2{}^+$ wave packets produced in the leading edge of the laser pulse can be trapped in the bond-hardened state near the peak region of the laser pulse. However, in the falling edge of the laser pulse, the upper state returns to be repulsive, and thus the wave packets can continue to dissociate. During the whole process, these wave packets will obtain a fraction of additional energy. This is a kind of dynamic Raman effect, in which the dissociated molecular ions absorb a higher-energy photon and re-emit a lower energy photon within the broad bandwidth of the ultrashort laser pulse. Therefore, the pulse shape and duration will have great effects on the process of gaining energy through the bond hardening. The extra absorbed photon energy during the dissociation is all allocated to the nuclei and the photoelectrons would not take away any additional energy. Therefore, the nondiagonal horizontal JES structures are formed at $\lambda = 790$ nm, which reveals there is no evident photoelectron-nuclear energy sharing structure. In the calculated photoelectron energy spectra shown in Figs. 5(e)

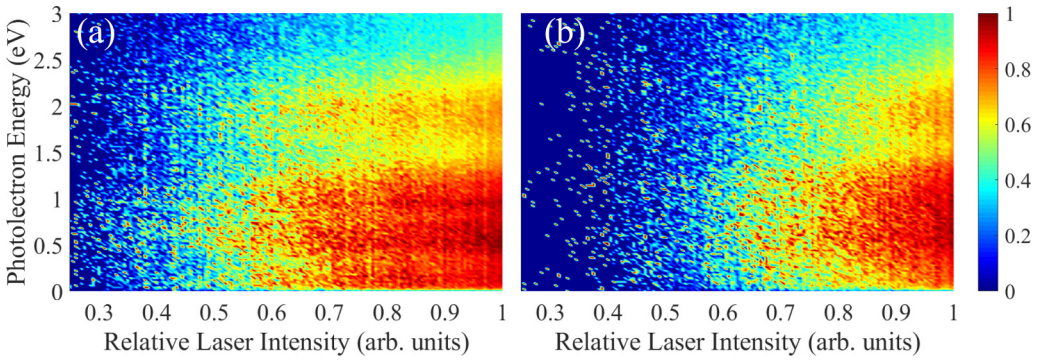

FIG. 6. The laser-intensity-dependent photoelectron energy spectra of the single ionization (a) and the dissociative ionization (b) channels at the wavelength of 790 nm.

and 5(f), the ATI structure seems difficult to be distinguished, revealing some limitations of our theoretical model. Note that, our model cannot reproduce the relative yield enhancement of photoelectrons near zero momentum of the single ionization if compared with the dissociative ionization channel.

We also note that the resonant electronic states of H_2 take important roles as well during multiphoton or tunneling ionization at $\lambda = 790$ nm. As seen in Fig. 6, one can clearly find that over a wide range of laser intensities, the peaks of the photoelectron energy spectra of the single ionization and the dissociative ionization channels do not change with respect to the laser intensity. This certainly means that in the process of dissociative ionization at $\lambda = 790$ nm, the H_2 molecule may first jump to its resonant states, which have a long life. The ionization of molecular ions will take place by absorbing more photons, subsequently. This will certainly result in the nondiagonal structure of JES at 790 nm. In addition, the focal volume effect of an actual laser pulse will also have influence on the JES. Since U_p is proportional to the laser intensity, the total energy of the nuclei and the photoelectron will distribute in a broad region because of different U_p corresponding to different intensities in the focus, which also makes the original back-diagonal lines in JES hard to be distinguished.

IV. CONCLUSIONS

In conclusion, we present a joint experimental and theoretical study on the laser wavelength and intensity dependence of the photoelectron-nuclear energy sharing mechanism for strong-field dissociative ionization of H_2. At $\lambda = 395$ nm, the distribution of the JES is found to change from a back-diagonal structure to a nondiagonal structure with the increase of the laser intensity, which can be explained by the deformation of the potential energy curves of H_2^+. On the contrary, at $\lambda = 790$ nm, bond hardening takes an important role in the energy sharing between the photoelectron and the nuclei during the molecular dissociation. The present investigations shed light on the complex photoelectron-nuclear dynamics in the laser-molecule interaction, which critically depends on the laser parameters. The coupled motion of the electron and the nuclei, together with the resonant electronic states and vibrational states of molecular ions during the multiphoton or tunneling ionization, make the photoelectron-nuclear energy sharing more complicated.

ACKNOWLEDGMENT

This work was supported by the NSFC (Grants No. 11434002, No. 11774013, and No. 11527901).

[1] P. Agostini, F. Fabre, G. Mainfray, G. Petite, and N. K. Rahman, Phys. Rev. Lett. **42**, 1127 (1979).
[2] P. H. Bucksbaum, A. Zavriyev, H. G. Muller, and D. W. Schumacher, Phys. Rev. Lett. **64**, 1883 (1990).
[3] L. J. Frasinski, J. H. Posthumus, J. Plumridge, K. Codling, P. F. Taday, and A. J. Langley, Phys. Rev. Lett. **83**, 3625 (1999).
[4] P. Lu, J. Wang, H. Li, K. Lin, X. Gong, Q. Song, Q. Ji, W. Zhang, J. Ma, H. Li, H. Zeng, F. He, and J. Wu, Proc. Nat. Acad. Sci. USA **115**, 2049 (2018).
[5] T. Zuo and A. D. Bandrauk, Phys. Rev. A **52**, R2511 (1995).
[6] J. Wu, M. Kunitski, M. Pitzer, F. Trinter, L. Ph. H. Schmidt, T. Jahnke, M. Magrakvelidze, C. B. Madsen, L. B. Madsen, U. Thumm, and R. Dörner, Phys. Rev. Lett. **111**, 023002 (2013).
[7] A. Lafosse, M. Lebech, J. C. Brenot, P. M. Guyon, O. Jagutzki, L. Spielberger, M. Vervloet, J. C. Houver, and D. Dowek, Phys. Rev. Lett. **84**, 5987 (2000).
[8] X. Sun, M. Li, Y. Shao, M.-M. Liu, X. Xie, Y. Deng, C. Wu, Q. Gong, and Y. Liu, Phys. Rev. A **94**, 013425 (2016).
[9] W. Zhang, Z. Li, P. Lu, X. Gong, Q. Song, Q. Ji, K. Lin, J. Ma, F. He, H. Zeng, and J. Wu, Phys. Rev. Lett. **117**, 103002 (2016).
[10] R. E. F. Silva, F. Catoire, P. Riviere, H. Bachau, and F. Martin, Phys. Rev. Lett. **110**, 113001 (2013).
[11] C. B. Madsen, F. Anis, L. B. Madsen, and B. D. Esry, Phys. Rev. Lett. **109**, 163003 (2012).
[12] H. Olivares-Pilón and A. V. Turbiner, Ann. Phys. **393**, 335 (2018).
[13] J. M. Peek, J. Chem. Phys. **43**, 3004 (1965).
[14] K. Pachucki, Phys. Rev. A **82**, 032509 (2010).
[15] J. Ullrich, R. Moshammer, A. Dorn, R. Dörner, L. Ph. H. Schmidt, and H. Schmidt-Böcking, Rep. Prog. Phys. **66**, 1463 (2003).

[16] Y. Mi, N. Camus, L. Fechner, M. Laux, R. Moshammer, and T. Pfeifer, Phys. Rev. Lett. **118**, 183201 (2017).
[17] J. H. Posthumus, B. Fabre, C. Cornaggia, N. de Ruette, and X. Urbain, Phys. Rev. Lett. **101**, 233004 (2008).
[18] X. Urbain, B. Fabre, E. M. Staicu-Casagrande, N. de Ruette, V. M. Andrianarijaona, J. Jureta, J. H. Posthumus, A. Saenz, E. Baldit, and C. Cornaggia, Phys. Rev. Lett. **92**, 163004 (2004).
[19] B. Fabre, J. H. Posthumus, V. Adrianarijaona, J. Jureta, and X. Urbain, Laser Phys. **13**, 964 (2003).
[20] B. Fabre, J. H. Posthumus, L. Malfaire, E. Staicu-Casagrande, J. Jureta, C. Cornaggia, E. Baldit, and X. Urbain, Laser Phys. **14**, 468 (2004).
[21] G. H. Dunn, J. Chem. Phys. **44**, 2592 (1966).
[22] M. E. Wacks, J. Res. Natl. Bur. Stand. Sect. A. **68A**, 631 (1964).
[23] D. B. Milošević, Phys. Rev. A **74**, 063404 (2006).
[24] H. Liang and L.-Y. Peng, Phys. Rev. A **101**, 053404 (2020).
[25] J. H. Posthumus, Rep. Prog. Phys. **67**, 623 (2004).
[26] H. Ibrahim, C. Lefebvre, A. D. Bandrauk, A. Staudte, and F. Légaré, J. Phys. B **51** (2018).
[27] B. Wu and Q. Niu, Phys. Rev. A **61**, 023402 (2000).
[28] Y. Liu, Y. Liu, and Q. Gong, Europhys. Lett. **101**, 68006 (2013).
[29] Y. Liu, Y. Liu, and Q. Gong, Phys. Rev. A **85**, 023406 (2012).